CMB anisotropies from acausal scaling seeds

Sandro Scodeller*
Institute of Theoretical Astrophysics, University of Oslo, PO Box 1029 Blindern, N-0315 Oslo, Norway

Martin Kunz†
Astronomy Centre, University of Sussex, Brighton BN1 9QH, UK and Département de Physique Théorique, Université de Genève, 24 quai Ernest Ansermet, CH–1211 Genève 4, Switzerland

Ruth Durrer‡
Département de Physique Théorique, Université de Genève, 24 quai Ernest Ansermet, CH–1211 Genève 4, Switzerland

(Dated: February 12, 2009)

We investigate models where structure formation is initiated by scaling seeds: We consider rapidly expanding relativistic shells of energy and show that they can fit current CMB and large scale structure data if they expand with super-luminal velocities. These acausally expanding shells provide a viable alternative to inflation for cosmological structure formation with the same minimal number of parameters to characterize the initial fluctuations. Causally expanding shells alone cannot fit present data. Hybrid models where causal shells and inflation are mixed also provide good fits.

PACS numbers: 98.80,11.30.Cp

I. INTRODUCTION

Inflationary models provide an excellent fit to all fluctuation data, the cosmic microwave background (CMB) anisotropies and polarization, as well as large scale structure data from galaxy catalogs. However, most current inflationary scenarios are simple toy models which are not well motivated from high energy physics. It is therefore not only justified, but important to study other ways to generate initial fluctuations.

In the past, especially models where topological defects act as seeds for fluctuations of the matter–radiation fluid have been studied. For simple global topological defects and for cosmic strings from the Abelian Higgs model, it has been found that they cannot reproduce the inflationary peak structure predicted by inflation [1, 2]. Comparison with present observations shows that topological defects can contribute at most about 10% to the CMB temperature fluctuations on large scales [3].

Since these competing models for structure formation have been ruled out, the general point of view in the field seems to be that only inflation can lead to a coherent series of acoustic peaks. However, this is not correct: Neil Turok and others have shown [4, 5] that a scaling seed model, where the seeds consist of a stochastic distribution of rapidly expanding shells of energy with a velocity close to the speed of light also leads to an acoustic peak structure like inflation. This "Turok model" was very promising in fitting CMB data back in 2001 [6]. However, there are arguments [7] that causal scaling seeds are not able to produce the a first peak in the E-polarization spectrum at $\ell \simeq 100$, which is due to polarization at the last scattering surface where this scale was super-horizon. As we show here, the Turok model with shells which expand with sub-luminal velocities (causal shells) indeed cannot fit the T-E correlation spectrum in present CMB data. However, this can be evaded if we allow for super-luminal expansion of the shells (acausal shells). As we shall see, acausal shells can generate CMB anisotropies and polarization as well as large scale structure which are in as good agreement with present data as inflationary models. They fit the WMAP 3 year [8] and ACBAR '08 [9] data as well as a simple inflationary model with the same number of parameters. Actually our simple model has three parameters to describe the seed perturbations, the amplitude and two velocities, however, as we shall see, two of them are strongly correlated, so that the parameter space is effectively two dimensional like in the simplest inflationary models (without gravitational waves and without running).

Super-luminal velocities are usually considered unphysical as they generically lead to signals which can propagate along a closed loop, see e.g. [10]. However, in the cosmological situation where we have a preferred Lorentz frame, the cosmological time, this conclusion can be avoided [11] since boost symmetry is broken. Even though one may not accept this argument on small scales, where physics should be independent of cosmological expansion, for cosmologically large objects like these expanding shells, super-luminal velocities cannot a priori be excluded.

In the remainder of this paper we show that super-

*Electronic address: sandro.scodeller@astro.uio.no
†Electronic address: m.kunz@sussex.ac.uk
‡Electronic address: ruth.durrer@unige.ch

luminally expanding shells can fit present CMB data as well as inflationary models can. In the next section we define and discuss our seed model. In Section III we present the results for the cosmological parameters as well as the primordial parameters for the pure seed model and the hybrid model. In the last section we draw some conclusions.

In this paper conformal time is denoted by t so that the metric is

$$ds^2 = a^2(t)\left(-dt^2 + \delta_{ij}dx^i dx^j\right) \ .$$

We set the spatial curvature to zero. Spacetime indices are lower case Greek letters and 3D spatial indices are lower case Latin letters. The conformal Hubble parameter is $\mathcal{H} = \dot{a}/a = aH$, where H denotes the physical Hubble parameter and a dot is a derivative w.r.t. conformal time t.

II. THE MODELS

We consider an inhomogeneous uncorrelated distribution of spherical expanding shells. The energy momentum tensor of uncorrelated spherical shells is purely scalar and we can parameterize it in the following way

$$T^0_0 = -\frac{M^2}{a^2} f_\rho \ , \tag{1}$$

$$T^i_j = \frac{M^2}{a^2}\left[f_p \delta^i_j + \left(\partial_i\partial_j - \frac{1}{3}\delta^i_j\Delta\right) f_\pi\right] \ , \tag{2}$$

$$T^0_i = \frac{M^2}{a^2}\partial_i f_v \ . \tag{3}$$

The energy density plus three times the pressure as well as the energy flux of the shells are posited to be

$$f_\rho(\mathbf{x},t) + 3f_p(\mathbf{x},t) = \sum_n \frac{\delta(|\mathbf{x}-\mathbf{z}_n| - v_1 t)}{4\pi\mathcal{H}t^{3/2}|\mathbf{x}-\mathbf{z}_n|^2} \ , \tag{4}$$

$$f_v(\mathbf{x},t) = -\sum_n \frac{3E(t)\theta(v_2 t - |\mathbf{x}-\mathbf{z}_n|)}{4\pi v_2^2 |\mathbf{x}-\mathbf{z}_n| t^{3/2}} \ . \tag{5}$$

Here the positions $\mathbf{z}_n$ are the centers of the exploding shells which are at random, uncorrelated positions. The function θ is the Heaviside function,

$$\theta(y) = \begin{cases} 1 & \text{if } y > 0 \\ 0 & \text{else,} \end{cases}$$

and the function $E(t)$ is given by

$$E(t) = \frac{4 - 2(\mathcal{H}t)^{-1}}{3 + 12\mathcal{H}t} \ .$$

To simplify the analysis we use infinitely thin shells for which the inner and outer radii coincide and expand with the same velocity. (This corresponds to the limit $B \to C$ in the original Turok model [4].) The above form of the energy momentum tensor ensures that the perturbations are of purely scalar nature. The two remaining functions in the parameterization of T^ν_μ are determined by energy and momentum conservation. The choice of $E(t)$, together with the factor $1/v_2^2$, assures that also f_π has compact support, $f_\pi(\mathbf{x},t) = 0$ if $|\mathbf{x}-\mathbf{z}_n| > vt$, where $v = \max(v_1, v_2)$. Then f_π has a white noise spectrum on large scales, $ktv < 1$. We assume that the centers $\mathbf{z}_n$ of the shells are uncorrelated and have a fixed comoving space density. Up to an irrelevant phase coming from the position of the shell center, the Fourier transforms of the source functions from one shell are given by

$$(f_\rho + 3f_p)(\mathbf{k},t) = \frac{1}{\mathcal{H}t^{3/2}}\frac{\sin(v_1 kt)}{v_1 kt} \ , \tag{6}$$

$$f_v(\mathbf{k},t) = \frac{3E(t)}{v_2^2 k^2 t^{3/2}}\left(\cos(v_2 kt) - \frac{\sin(v_2 kt)}{v_2 kt}\right) . \tag{7}$$

As the different shells are uncorrelated, their contributions can be added with random phases. In the limit of many uncorrelated shells, the spectra of $f_\rho + 3f_p$ and f_v are then simply the squares of the above functions, e.g.,

$$\langle f_v(\mathbf{k},t) f_v^*(\mathbf{k}',t)\rangle = (2\pi)^3\delta(\mathbf{k}-\mathbf{k}')P_v(k,t) \tag{8}$$

with

$$P_v(k,t) = A^2\frac{9E^2(t)}{v_2^4 k^4 t^3}\left(\cos(v_2 kt) - \frac{\sin(v_2 kt)}{v_2 kt}\right)^2 , \tag{9}$$

$$= A^2 |f_v(k,t)|^2 . \tag{10}$$

The constant pre-factor A determines the number of shells per Hubble volume.

In Fourier space energy and momentum conservation require

$$\dot{f}_\rho + k^2 f_v + \mathcal{H}(f_\rho + 3f_p) = 0 \, , \tag{11}$$

$$\dot{f}_v + 2\mathcal{H}f_v - f_p + \frac{2}{3}k^2 f_\pi = 0 \, . \tag{12}$$

Integrating the first equation one finds *e.g.* during the radiation dominated era when $\mathcal{H}t = 1$, so that $E(t) = 2/15$,

$$f_\rho = \frac{4}{3\sqrt{t}}\Big\{\Big[\cos(v_1 kt) + \frac{\sin(v_1 kt)}{2v_1 kt} + \sqrt{2\pi v_1 kt}\, S\left(\sqrt{\frac{2v_1 kt}{\pi}}\right)\Big] + \frac{1}{5v_2^2}\Big[\cos(v_2 kt) - \frac{\sin(v_2 kt)}{v_2 kt} + \sqrt{2\pi v_2 kt}\, S\left(\sqrt{\frac{2v_2 kt}{\pi}}\right)\Big]\Big\} . \tag{13}$$

$$
\begin{aligned}
f_\pi \;=\; & \frac{1}{k^2\sqrt{t}}\Big\{\frac{3}{10}\Big[2\frac{\sin(v_2kt)}{v_2kt}+\frac{\cos(v_2kt)}{(v_2kt)^2}-\frac{\sin(v_2kt)}{(v_2kt)^3}\Big] \\
& -\frac{2}{15v_2^2}\Big[\cos(v_2kt)-\frac{\sin(v_2kt)}{v_2kt}+ \\
& \sqrt{2\pi v_2kt}S\left(\sqrt{\frac{2v_2kt}{\pi}}\right)\Big] \\
& -\frac{2}{3}\Big[\cos(v_1kt)-\frac{1}{4}\frac{\sin(v_1kt)}{v_1kt}+ \\
& \sqrt{2\pi v_1kt}S\left(\sqrt{\frac{2v_1kt}{\pi}}\right)\Big]\Big\}\,. \qquad (14)
\end{aligned}
$$

Here $S(x)$ denotes the sine Fresnel integral as defined in [12]. A similar result is obtained during the matter era. Even though this is not directly evident, a series expansion shows that f_π is white noise for small arguments, $kt \ll 1$, as it should be for the Fourier transform of a function with compact support. The source function f_p is easily determined with the help of Eqs. (6) and (13). The metric perturbations due to the shells are given by the seed Bardeen potentials [13]

$$
\begin{aligned}
k^2\Phi_s &= \epsilon(f_\rho + 3\mathcal{H}f_v)\,, && (15)\\
\Psi_s &= -\Phi_s - 2\epsilon f_\pi\,, && (16)\\
\text{where}\quad \epsilon &= 4\pi G M^2 A \ll 1 && (17)
\end{aligned}
$$

determines the overall amplitude. The matter Bardeen potentials on the other hand are given by the matter density perturbations and anisotropic stresses,

$$
\begin{aligned}
k^2\Phi_m &= 4\pi G a^2 \rho D\,, && (18)\\
k^2(\Phi_m+\Psi_m) &= 8\pi G a^2 p\Pi\,, && (19)
\end{aligned}
$$

where Π denotes the anisotropic stress of the cosmic fluid and D is a gauge invariant density perturbation variable. Care is required when relating D to the density fluctuation in longitudinal gauge since then a term proportional to the total Bardeen potential $\Phi = \Phi_s + \Phi_m$ enters the equation. More details can be found in Refs. [6, 14]. The total Bardeen potentials,

$$
\Phi = \Phi_s + \Phi_m \;,\; \text{and} \qquad \Psi = \Psi_s + \Psi_m \qquad (20)
$$

then enter the usual evolution equation for cosmic matter and radiation.

We shall now show that even though current CMB data cannot be fitted with expanding shells as long as we require causality, when allowing for super-luminal expansion we can obtain excellent fits which rival the fits from inflationary models to all data. We shall also comment on mixed models.

The seed perturbations from expanding shells are determined by the velocities v_1 and v_2 and an amplitude ϵ which is proportional to the number density of shells. However, the amplitude needed to obtain a good fit is tightly correlated with v_1, as we shall discuss below and as is shown in Fig. 1. Once the best fit value of v_1 is determined, the amplitude is effectively fixed. Therefore, expanding shells can be regarded as models requiring effectively two parameters for the initial fluctuations, like scalar inflationary perturbations.

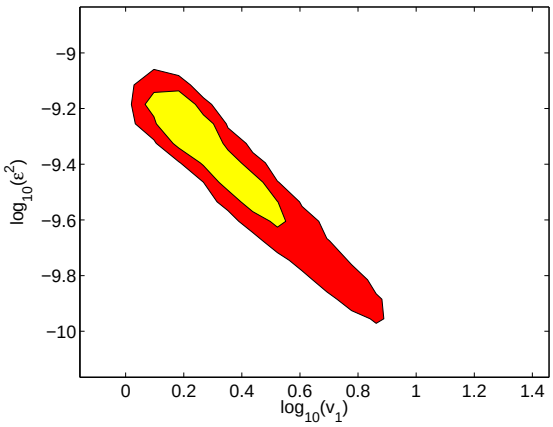

FIG. 1: A 2D likelihood plot showing the degeneracy between the velocity v_1 and the amplitude ϵ^2. The yellow colored area encloses 68% and the larger red colored area 95% of the likelihood volume (marginalized over all other parameters).

For the mixed models, we add scalar fluctuations from inflation which are characterized by the amplitude A_s and the scalar spectral index n_s, $\langle|\Phi_m(t_{\rm in},k)|^2k^3\rangle \simeq \langle|\Psi_m(t_{\rm in},k)|^2k^3\rangle = A_s(k/k_0)^{(n_s-1)}$, where $k_0 = 0.002{\rm Mpc}^{-1}$ is the pivot scale. We assume the inflationary perturbations to be uncorrelated with the seeds (expanding shells).

III. RESULTS

We start by investigating models where perturbations are generated purely from the expanding shells. A first interesting result is that this model cannot provide a good fit to CMB data if we constrain $v_1 \leq 1$ and $v_2 \leq 1$. We can obtain reasonable, but not sufficiently good fits for the temperature anisotropy, see Fig. 2; but we cannot fit the polarization data. This is seen especially well when comparing the model with the high quality TE correlation data from WMAP [8], see Fig. 3.

Also the pure polarization spectrum differs from the inflationary polarization by the absence of the first, acausal peak at $\ell \simeq 130$, see Fig. 4. However, the current observations of the EE spectrum are not sufficiently accurate on large scales to rule out the absence of a peak at $\ell \simeq 130$.

We have used the code CMBEASY [20] and its Monte Carlo Markov Chain (MCMC) analysis tool [21] to determine the best fit cosmological parameters for a spatially flat cosmology with photons, massless neutrinos, cold dark matter and a cosmological constant. For the fitting procedure we used the 3 year WMAP data [8, 18], the Boomerang 2003 data [15], the CBI [16] and the old ACBAR data [17], as well as the Sloan Digital Sky Survey

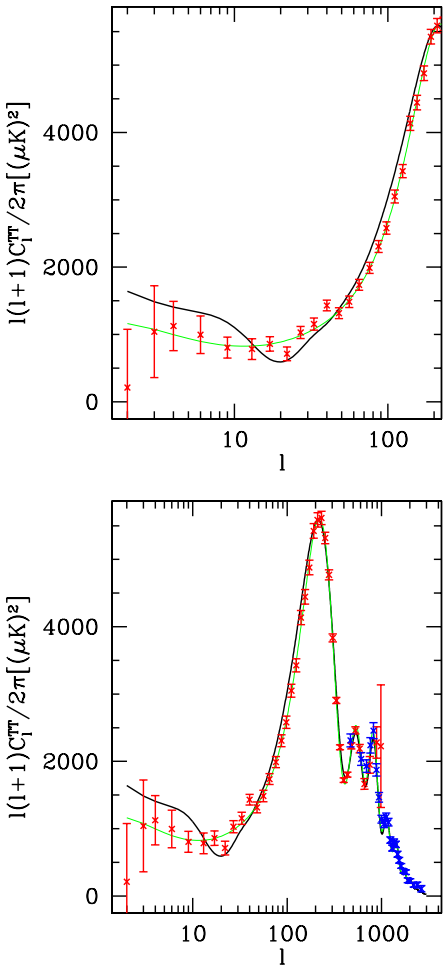

FIG. 2: The best fit CMB anisotropies from a **causal** model of expanding shells is shown (fat black line) and compared with the data from WMAP and ACBAR, and to the best fit ΛCDM model (thin green line). The top panel shows the rise to the first peak, $\ell \leq 200$ which can not be fitted satisfactorily by this model. The bottom panel shows the spectrum up to $\ell = 2500$. The secondary peaks are well fitted. The parameter values for the best fit causal shell model are given in the text.

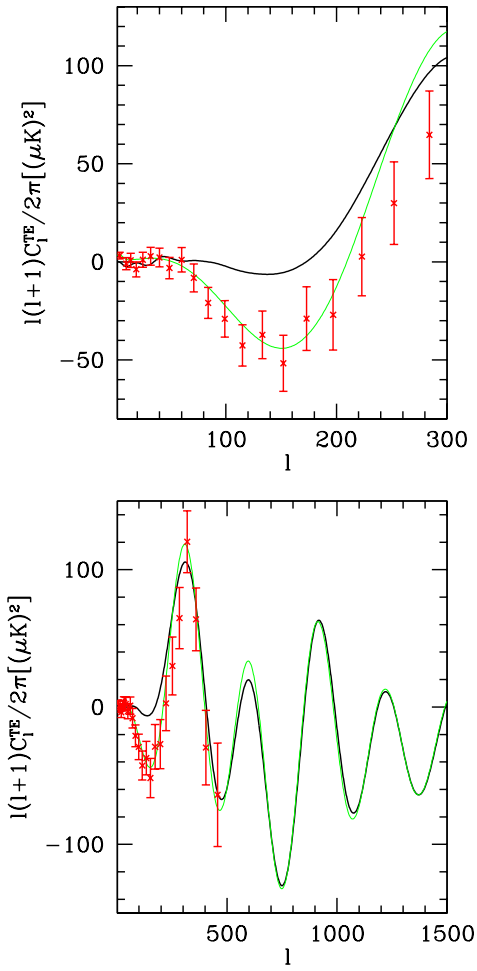

FIG. 3: The best fit T-E correlation spectrum from a **causal** model of expanding shells (fat black line) is compared with the data from WMAP and with a standard ΛCDM model (thin green line). The top panel shows the first acausal anti-correlation peak, at $\ell \simeq 150$ which is absent in the causal model, while the bottom panel shows the spectrum up to $\ell = 1500$. The secondary peaks are very similar to the inflationary case. The parameter values are the same as for Fig. 2.

(SDSS) power spectrum for luminous red galaxies [19], which is supposed to be still in the linear regime. In the figures the best fit solution for the CMB anisotropies are compared with the 3 year WMAP data [8, 18] and with the recent ACBAR results [9].

The maximum of the likelihood for the causal models has quite a complicated structure, with several peaks close together. The best-fitting model which we could find has the following parameter values: a Hubble parameter $H_0 = 100h$km/s/Mpc where $h = 0.686$, a matter density parameter $\Omega_m h^2 = 0.137$, a baryon density parameter $\Omega_b h^2 = 0.0220$, an optical depth $\tau = 0.36$, shell velocities $v_1 = 0.77$, $v_2 = 1.0$ and the amplitude $10^{10}\epsilon^2 = 26.0$. Most cosmological parameters are similar to their values for inflationary perturbations. The best fit parameters for a simple inflationary model fitted to the same data are $h = 0.713$, $\Omega_m h^2 = 0.133$, $\Omega_b h^2 = 0.0223$, $\tau = 0.08$, $n_s = 0.956$ and $A_s = 2.3 \times 10^{-9}$.

The best fit optical depth for the causal seed model is larger than in the inflationary models. In order to generate T-E correlations on large scales, the optical depth tends to increase. It might be possible to motivate a larger value of τ if the shells could initiate reionization. Also the best fit velocity v_2 is at the upper limit of the prior and would prefer to exceed the causality limit. Our MCMC chains had severe difficulties to converge for this model, which is partly due to the fact that the best fit lies at the boundary of the priors for several parameters, which seems to cut a connected acausal best-fit region up into several unconnected causal ones. We can there-

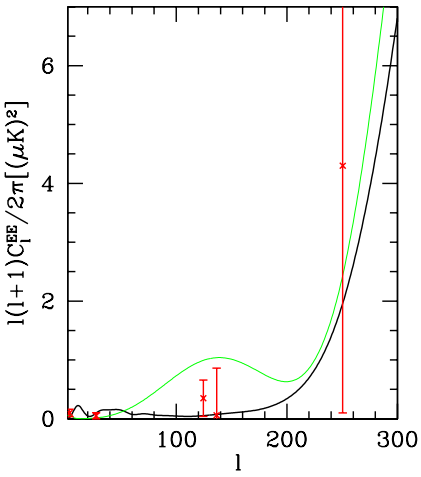

FIG. 4: The best fit EE power spectrum from a **causal** model of expanding shells (fat black line) is compared with the data from WMAP and with a standard ΛCDM model (thin green line). Only the region of the first acausal peak, $\ell \leq 300$ is shown, where the causal model differs from inflation. The secondary peaks are very similar to the inflationary case. The parameter values are the same as for Fig. 2.

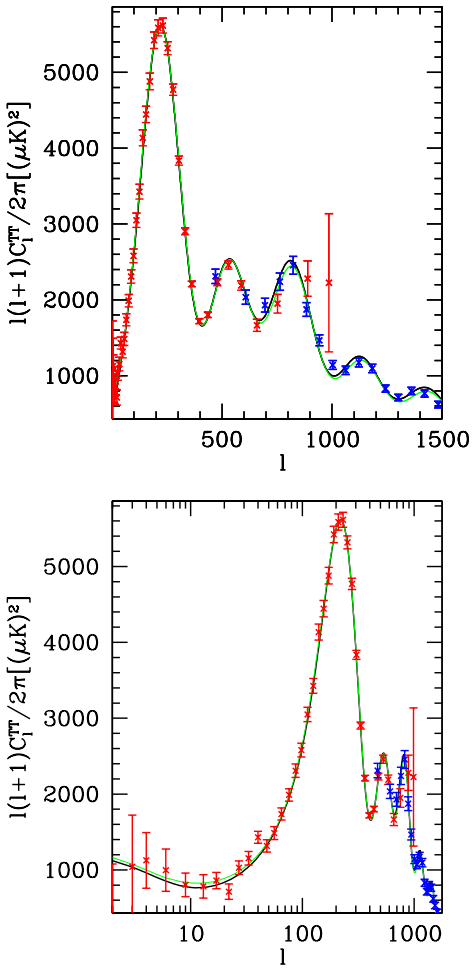

FIG. 5: The best fit CMB anisotropies from an **acausal** seed model are shown (fat black line) and compared with the data from WMAP and ACBAR and to a standard ΛCDM model (thin green line). The top panel uses a linear scale in ℓ while the bottom panel used log scaling to emphasize the Sachs–Wolfe plateau at low values of ℓ. The best fit parameter values used for this plot are given in Table I.

fore not say that a velocity $v_1 < 1$ is significantly preferred since there is a second maximum with $v_1 \approx 1$ and $v_2 \approx 0.7$ which seems to have $\Delta\chi^2 = 20$ with respect to the best-fit models, but which is completely disconnected from the first maximum so that no chains have managed to sample both. We are also reluctant to quote 1-sigma errors, first of all since the MCMC chains did not converge well, and secondly since the model is not a good fit and hence error-bars are not useful.

Only if we allow for super-luminal expansion of the shells can we obtain a good fit to present data. The best fit cosmological parameters for super-luminally expanding shells obtained using the same data are surprisingly close to those for an inflationary ΛCDM model: We find $\Omega_m h^2 = 0.134$, $\Omega_b h^2 = 0.0232$, $h = 0.745$, $\tau = 0.11$. The best fit model parameters are $v_1 = 1.65$ and $v_2 = 5.66$. The amplitude is inversely proportional to $\sqrt{v_1}$ and the CMB normalization requires $\epsilon^2 v_1 = 9.4 \times 10^{-10}$, see Fig. 1. For the above value of v_1 we therefore infer $\epsilon^2 = 5.7 \times 10^{-10}$.

Even though the recent ACBAR data has not been used in the fitting procedure, our best fit anisotropies shown in Fig. 5 do reproduce it nicely.

In Fig. 6 we show the T-E-polarization cross correlation for this model and compare it with the data and with the result for a standard ΛCDM model. As one already sees by eye, within the accuracy of present data both models fit equally well. The same is true for the E-polarization spectrum shown in Fig. 7. Since the perturbations are purely scalar there is no B-polarization.

It is interesting to note that the first polarization peak at $\ell \simeq 130$ is also reproduced by the seed model. According to [7] this is only possible since the explosions are super-luminal, $v_{1,2} > 1$. This is exactly what we see. As long as both velocities are below the speed of light, $v_1, v_2 \leq 1$, the first polarization peak remains absent, see Fig. 4. When the velocities exceed the speed of light, the peak starts building up. In order to match the observed T-E anti-correlation, which is in inflationary models due to a superposition of a cosine wave (from the adiabatic density mode) and a sine wave (from the velocity mode) and appears for $kt_{\rm dec} \approx 0.66$ we need a velocity $v \gtrsim 1/(kt_{\rm dec}) \approx 1.5$ at decoupling, which agrees well with the point at which the expanding shell model becomes acceptable. It is also interesting to note that the spectra do not depend on v_2 any more once it exceeds about $v_2 \sim 6$. This can be seen in the likelihood

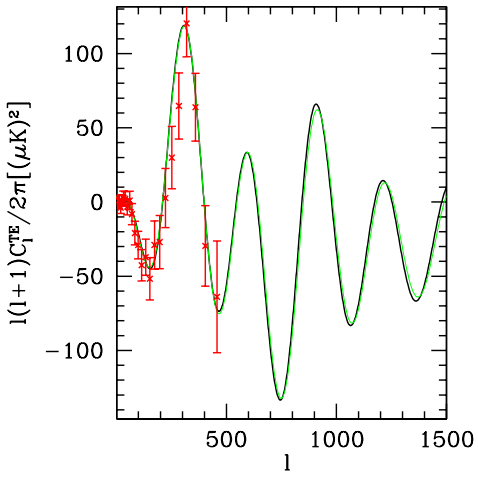

FIG. 6: The cross correlation spectrum of temperature anisotropy and E-polarization from a pure seed model is shown (fat black line) and compared with the WMAP data given in Ref. [18] (we did not plot the data with $\ell > 500$ because of its large error bars). The best fit ΛCDM curve is also indicated (fine green line) but is nearly invisible since it coincides nearly perfectly with the seed model curve. The parameter values are the same as for Fig. 5.

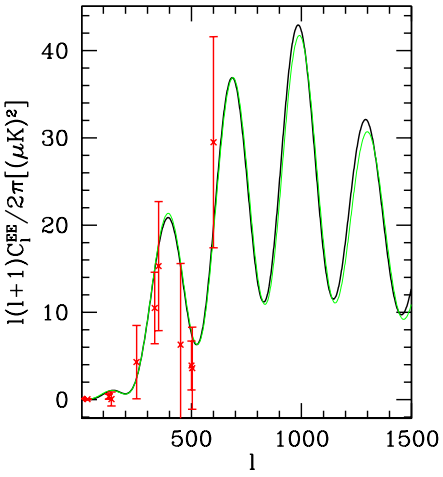

FIG. 7: The E-polarization from a pure seed model is shown (fat black line) and compared with the data from DASI, Boomerang-2003 and WMAP as given in Ref. [18]. The best fit ΛCDM polarization curve is also indicated (fine green line). The parameter values are the same as for Fig. 5.

plot Fig. 8. The likelihood plots for cosmological parameters are quite similar to the ones from inflation. For completeness we show some of them in the appendix.

In Table I we summarize the results for the acausal expanding shells model. The best-fit likelihood is slightly below the one of the best-fit inflationary model with $\Delta \ln \mathcal{L} = 2.3$. We expect that this could be further improved, at the expense of introducing more parameters, e.g. by allowing for a different evolution in matter and

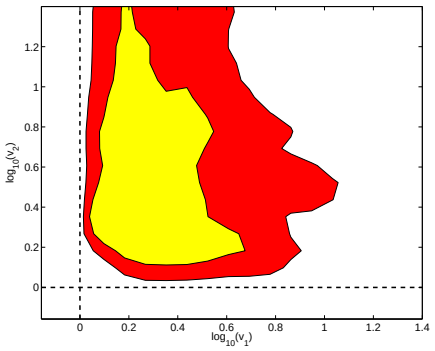

FIG. 8: The 2-parameter likelihood plot for (v_1, v_2) is shown (68% and 95% confidence contours). Both velocities have to be larger than 1. v_1 has a preference for $v_1 \approx 1.6$ while v_2 has no strong upper limit.

radiation domination beyond the simple factor $1/(\mathcal{H}t)$ in Eq. (5), or by allowing the shell velocities to change with time.

v_1	v_2	$10\Omega_m h^2$	$10\Omega_b h^2$	H_0	τ
$1.65^{+7.1}_{-0.35}$	$5.66^{+\infty}_{-4.26}$	$1.34^{+0.07}_{-0.08}$	$0.23^{+0.01}_{-0.01}$	75^{+3}_{-3}	$0.11^{+0.07}_{-0.04}$

TABLE I: Best-fit values and 95% symmetric confidence intervals for the acausally expanding shell model. The best fit likelihood is $\ln \mathcal{L} = -1750.4$; slightly worse than the for simple inflationary models with the same number of parameters where we find $\ln \mathcal{L} = -1748.1$.

In our MCMC we have also fitted the power spectrum of luminous red galaxies (LRG) as given in [19]. The best fit power spectra are compared with the data in Fig. 9, for the causal and acausal shell models as well as for inflation. On super-horizon scales, $k \lesssim 10^{-3} h\mathrm{Mpc}^{-1}$, the power spectrum of the causal model is severely suppressed. Of course, there is no data available on these scales.

If we require causality, $v_1, v_2 \leq 1$, we cannot fit the CMB data with a pure seed model. However a mixture of expanding shells and inflation can provide a good fit. Due to problems in the MCMC for the hybrid model, we do not have much statistics, so not all best fit parameters from the likelihood-analysis are converged values. The best fit parameters which we found for a hybrid model with flat spatial sections are

$$\begin{aligned} 10^{10}\epsilon^2 &= 1.20\,, \quad & v_1 &= 0.80\,, \quad & v_2 &= 0.77\,, \\ 10^{10} A_s &= 20.02\,, \quad & n_s &= 0.95\,, & & \\ \Omega_m h^2 &= 0.131\,, \quad & \Omega_b h^2 &= 0.0217\,, \quad & h &= 0.70\,. \end{aligned}$$

In Fig. 10 we show the two parameter likelihood for the shell velocities and the one parameter likelihood for the

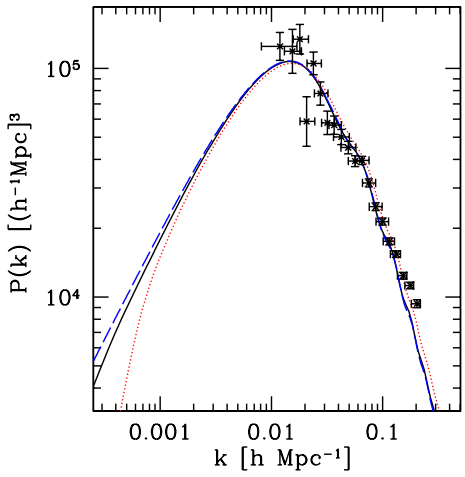

FIG. 9: The power spectra from causal expanding shells (dotted, red), acausal expanding shells (solid, black) and inflation (dashed, blue) are compared with data from luminous red galaxies [19]. In the observable region, the acausal shell and inflationary power spectra are indistinguishable.

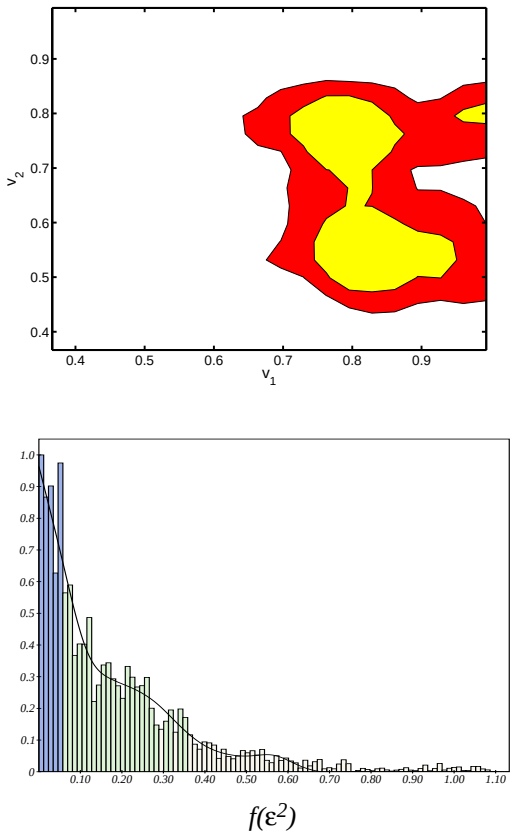

FIG. 10: The 2-parameter likelihood plot for (v_1, v_2) is shown for the mixed model with expanding shells and inflation (top). In the bottom panel we also show the likelihood distribution for $f\left(\epsilon^2\right) = \ln \epsilon^2 - 2\tau$.

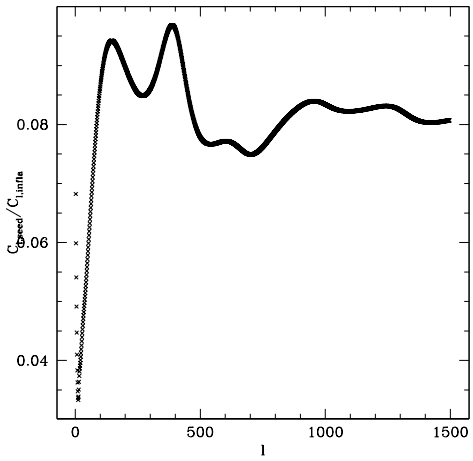

FIG. 11: The ratio $\frac{C^{TT}_{\ell,\mathrm{seed}}}{C^{TT}_{\ell,\mathrm{infla}}}$ for the best-fit hybrid model.

amplitude ϵ^2. The likelihood for ϵ^2 peaks close to zero, which seems to indicate that the data prefers a vanishing contribution from the shells. Surprisingly for such a small amplitude (compared to the amplitude A_s of the inflationary part) the contribution of the shells is non-negligible, this can be seen by looking at the ratio of the C_ℓ from shells and from inflation; see Fig. 11.

As can also be seen for the best-fit causal model in Fig. 2, the shells have a minimal contribution to the temperature anisotropies at $\ell \approx 10$ so they do not contribute much at the Sachs-Wolfe plateau, but their contribution amounts to $\sim 10\%$ at higher ℓ, as shown in Fig. 11.

In all, this mixed model is is similar to models mixing inflation with topological defects. It is a logical possibility, but does not seem very attractive since it increases the number of parameters with only a marginal enhancement of the likelihood of the model.

IV. CONCLUSIONS

In this work we have revisited models with seeds, comparing them with recent CMB data. We have specifically analyzed a model proposed by Neil Turok [4], where the seeds are rapidly expanding spherical shells. We have found that a seed model with sub-luminal velocities cannot fit the CMB data.

However, if we allow for super-luminal explosion speeds, acausal shells, we can find an excellent fit to CMB anisotropies and polarization as well as to the linear matter power spectrum. It is intriguing that the velocities do not need to be *much* larger than the speed of light, just $v \gtrsim 1.5c$ is already sufficient. This model has effectively the same number of parameters (two) as the simplest inflationary model with purely scalar perturbations.

The power spectra are so similar to the inflationary ones that it is not clear, at least on the level of linear perturbations, how this model could be distinguished from inflationary perturbations. One possibility might be via a tensor component. Even though slight deviations from spherical symmetry might also lead to a tensor component for the expanding shell model, this component will probably not have the same characteristics as a tensor component from slow roll inflation (e.g. the consistency relation between the tensor to scalar ratio and the tensor spectral index).

Super-luminal explosions do seem somewhat unphysical. Nevertheless, it has been argued [11] that superluminal speeds in cosmology do not lead to serious acausalities since Lorentz invariance is broken in a Friedmann-Lemaître universe, where the cosmological reference frame represents a preferred frame. Although this seems quite artificial on small scales, the argument may be valid on the cosmologically large scales of these expanding shells. It might therefore be advisable to keep an open mind. especially when considering that inflation is usually implemented with the help of the potential energy of a scalar field, the normalization of which is intimately linked to the cosmological constant, the probably biggest unsolved problem in cosmology.

We have also investigated hybrid models with seeds and inflationary perturbations. Good fits are obtained with seed contributions of about 10% on angular scales, $\ell \gtrsim 100$.

Acknowledgments

This work is supported by the Swiss National Science Foundation. Ruth and Sandro thank Sussex University for hospitality. The numerical computations have been performed on the Myrinet cluster of Geneva University and Archi cluster of the University of Sussex.

Appendix A: Likelihoods

In this appendix we show some additional likelihood plots for the parameters of the acausal expanding shell model discussed in this work. For the 1D likelihoods, the (blue) solid line always shows the marginalized likelihood of the acausal model while the (red) dashed curve is the marginalized likelihood for the inflationary case. In Fig. 12 one sees that the cosmological parameters obtained for the acausal seed model are quit similar to inflationary parameters. Even though the best fit $\Omega_b h^2$, h and τ for the seed model are somewhat higher, the inflationary best fit value is within one sigma.

In Fig. 13 the 1 dimensional likelihoods for the velocities are shown. Clearly, once the velocities are above about 1.5, the fit becomes good. For v_1 the likelihood decreases steeply above about $v_1 = 3$ (albeit with a long tail) while it remains nearly constant for v_2 which therefore seems not to have an upper bound. We have also found that above $v_2 \sim 6$ the spectra are nearly independent of the value of v_2.

[1] R. Durrer, A. Gangui and M. Sakellariadou, Phys. Rev. Lett. **76**, 579 (1996) [arXiv:astro-ph/9507035].
[2] C. Contaldi, M. Hindmarsh and J. Magueijo, Phys. Rev. Lett. **82**, 679 (1999) [arXiv:astro-ph/9808201].
[3] N. Bevis, M. Hindmarsh and M. Kunz, Phys. Rev. **D70**, 043508 (2004) [arXiv:astro-ph/0403029];
N. Bevis, M. Hindmarsh, M. Kunz and J. Urrestilla, Phys. Rev. **D75**, 065015 (2007) [arXiv:astro-ph/0605018].
[4] N. Turok, Phys. Rev. Lett. **77**, 4138 (1996) [arXiv:astro-ph/9607109].
[5] W. Hu, D. Spergel and M. White, Phys. Rev. **D55**, 3288 (1997) [arXiv:astro-ph/9605193].
[6] R. Durrer, M. Kunz and A. Melchiorri, Phys. Rev. **D63**, 081301(R) (2001) [arXiv:astro-ph/0010633].
[7] D. Spergel and M. Zaldarriaga, Phys. Rev. Lett. **79**, 2180 (1997) [arXiv:astro-ph/9705182].
[8] G. Hinshaw et al., Astrophys. J. Suppl. **170**, 288 (2007) [arXiv:astro-ph/0603451].
[9] C. Reichardt et al., arXiv:0801.1491v2
[10] C. Bonvin, C. Caprini and R. Durrer, arXiv:0706.1538 (2007).
[11] E. Babichev, V. Mukhanov and A. Vikman (2007) [arXiv:0708.0561].
[12] M. Abramowitz and I Stegun, *Handbook of Mathematical Functions, tenth Edition*, Dover Publications (New York, 1970).
[13] R. Durrer, Phys. Rev. **D42**, 2533 (1990).
[14] S. Scodeller, Master thesis at Geneva University (2007).
[15] W.C. Jones et al., Astrophys.J. **647**, 823 (2006) [arXiv:astro-ph/0507494].
[16] A.C.S. Readhead et al., Astrophys. J. **609**, 498 (2004) [arXiv:astro-ph/0402359].
[17] C.L. Kuo et al., Astrophys. J. **600**, 32 (2004) [arXiv:astro-ph/0212289].
[18] L. Page et al., Astrophys. J. Suppl. **170**, 335 (2007) [arXiv:astro-ph/0603450].
[19] M. Tegmark et al., Phys. Rev. **D 74**, 123507 (2006) [arXiv:astro-ph/0608632].
[20] M. Doran, JCAP **0510**, 011 (2005) [arXiv:astro-

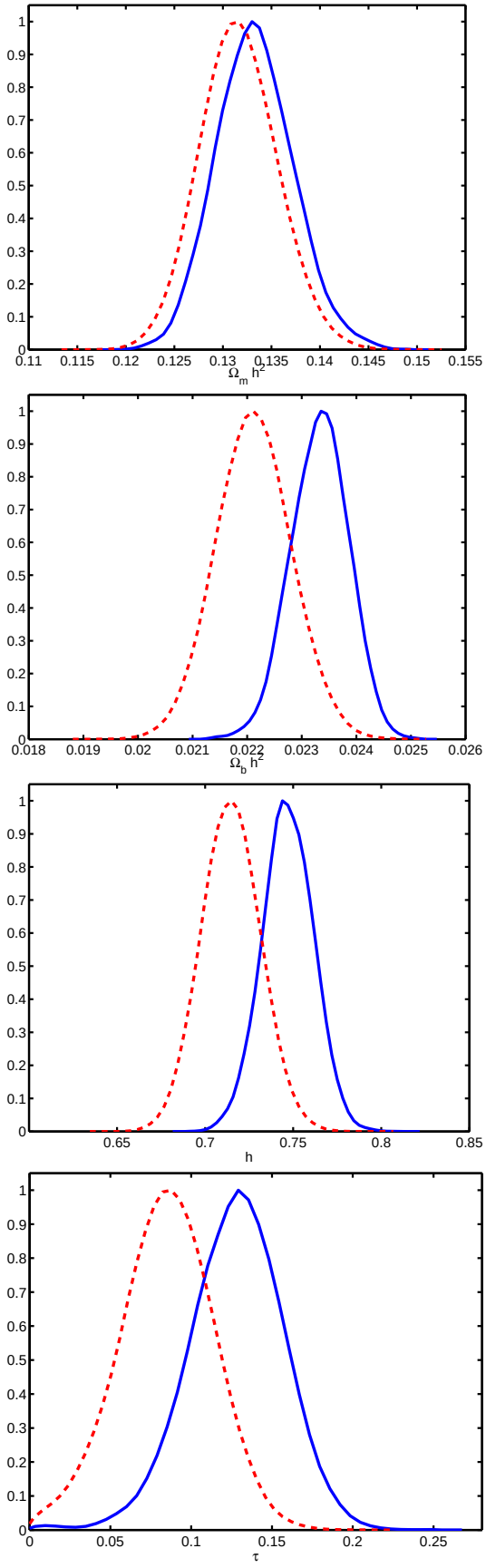

FIG. 12: The 1D likelihood plots for the acausal model (blue solid line) and the standard inflationary case (red dashed line). The top-left panel shows $\Omega_m h^2$, the top right panel $\Omega_b h^2$, the lower left panel h and the lower right panel τ.

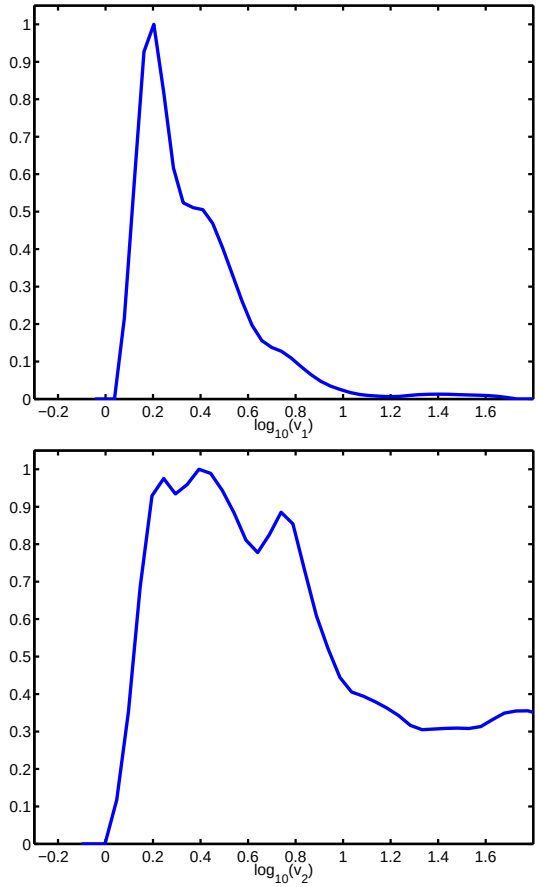

FIG. 13: The 1D likelihood plots for the velocities in the acausal model: The left panel shows $\log_{10}(v_1)$ and the right panel $\log_{10}(v_2)$. v_1 shows a preference for $v_1 \approx 1.5$ with a long tail to higher velocities, while v_2 is basically unconstrained apart from $v_2 > 1$.

ph/0302138], www.cmbeasy.org.
[21] M. Doran and C.M. Müller, JCAP **0409**, 003 (2004) [arXiv:astro-ph/0311311].